

Zero kinetic energy photoelectron spectroscopy of jet cooled benzo[*a*]pyrene from resonantly enhanced multiphoton ionization

Jie Zhang, Colin Harthcock, Fangyuan Han, and Wei Kong^{a)}

Department of Chemistry, Oregon State University, Corvallis, Oregon 97331-4003, USA

(Received 12 September 2011; accepted 5 December 2011; published online 28 December 2011)

We report zero kinetic energy (ZEKE) photoelectron spectroscopy of benzo[*a*]pyrene (BaP) via resonantly enhanced multiphoton ionization (REMPI). Our analysis concentrates on the vibrational modes of the first excited state (S_1) and those of the ground cationic state (D_0). Similar to pyrene, another peri-condensed polycyclic aromatic hydrocarbon we have investigated, the first two electronically excited states of BaP exhibit extensive configuration interactions. However, the two electronic states are of the same symmetry, hence vibronic coupling does not introduce any out-of-plane modes in the REMPI spectrum, and Franck-Condon analysis is qualitatively satisfactory. The ZEKE spectra from the in-plane modes observed in the REMPI spectrum demonstrate strong propensity in preserving the vibrational excitation of the intermediate state. Although several additional bands in combination with the vibrational mode of the intermediate state are identifiable, they are much lower in intensity. This observation implies that the molecular structure of BaP has a tremendous capability to accommodate changes in charge density. All observed bands of the cation are IR active, establishing the role of ZEKE spectroscopy in mapping out far infrared bands for astrophysical applications.

© 2011 American Institute of Physics. [doi:10.1063/1.3672161]

INTRODUCTION

Polycyclic aromatic hydrocarbons (PAHs) are a group of hydrocarbon molecules with fused six member aromatic ring frames terminated with peripheral hydrogen atoms. They are an important group of molecules for laboratory astrophysical studies because of their possible role in infrared (IR) emission in the interstellar medium (ISM) and their potential as an energy and carbon storage reservoir.¹⁻⁷ In the mid 1970s, a series of unidentified infrared (UIR) bands, including features at 3.3, 6.2, 7.7, 8.6, and 12.7 μm , have been discovered in a spectroscopic study of planetary nebulae.¹ Later on, these UIR bands have been shown to be ubiquitous for a variety of astronomical sources. It is well accepted now that these 3.3–17.4 μm features can be characterized as C–H, C–C, or C–C–C stretching modes.²⁻⁷ PAHs have since been considered an important subject of astrophysical investigations. Given the abundant radiation sources in the ISM, ionic PAHs have also been considered promising carriers of the UIR bands.⁸⁻¹⁰

For comparisons with astrophysical observations, efforts have been made on the study of laboratory IR spectroscopy of PAHs and their cations, including matrix isolation spectroscopy,^{11,12} IR emission,¹³ laser induced fluorescence, photoionization spectroscopy,¹⁴ and cavity ringdown spectroscopy.¹⁵ Unfortunately, identification of specific PAHs has been unsuccessful so far, largely due to the fact that mid-IR bands only represent local motions or functional groups of a molecule. In contrast, far-infrared (FIR) bands are sensitive to the molecular size and structure; hence, FIR spectroscopy is considered “fingerprint” of individual molecule or ion. The

Herschel Space Observatory launched in May, 2009 is aimed for the FIR and submillimeter wavelength region of the ISM. One of the goals of *Herschel* is to map out the chemical composition of the ISM and the atmospheres and surfaces of comets, planets, and satellites.

Laboratory FIR spectroscopy has always been challenging due to the lack of light sources and detectors. Moreover, spectroscopy of ions is further hindered by the low achievable particle density. The technique of zero kinetic energy (ZEKE) photoelectron spectroscopy serves as an ideal tool, albeit indirect, for the study of low frequency vibrational modes of cations.¹⁶⁻¹⁸ ZEKE is known for its high resolution of cation rovibrational spectroscopy. The high Rydberg states in ZEKE are longer lived when they are associated with lower vibronic states of the cation, and this feature makes ZEKE particularly suitable for studies of lower frequency vibrational modes. Thus, by detecting electrons from pulsed field ionization in ZEKE spectroscopy via resonantly enhanced multiphoton ionization (REMPI), we can avoid both the light source and the detector problems in typical FIR and submillimeter wave experiments. The vibrational information from ZEKE is largely governed by the Franck-Condon (FC) principle, hence the information from ZEKE might not be directly applicable for line identification in astronomy, but the information of IR inactive modes can be used for frequency calibrations of FIR spectroscopy from theoretical calculations and for modeling of the energy and chemical balance in the ISM.^{19,20}

Benzo[*a*]pyrene (BaP) is a five ring PAH as shown in Figure 1. It is the most abundant PAH in the earth’s atmosphere and it is highly carcinogenic.²¹⁻²³ Although it has been more than seventy years since the first study of BaP,²⁴ spectroscopic information is still limited. Imasaka *et al.*²⁵ performed

^{a)} Author to whom correspondence should be addressed. Electronic mail: wei.kong@oregonstate.edu. Fax: 541-737-2062.

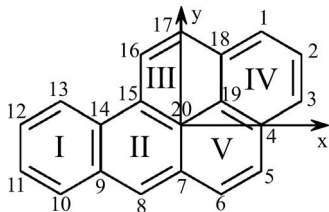


FIG. 1. Structure of benzo[*a*]pyrene and definition of the molecular coordinate system.

the first fluorescence excitation spectrum in a supersonic jet and identified the origin of the first electronically excited state S_1 around 393 nm. Greenblatt *et al.*²⁶ later determined the origin of the $S_1 \leftarrow S_0$ transition at $25265 \pm 20 \text{ cm}^{-1}$ and measured the lifetime of the first excited state to be 270 ns. The authors further discussed the second excited state S_2 which was considered to be 1500 cm^{-1} higher than S_1 , and attributed the long lifetime of the S_2 state to strong vibronic coupling with the S_1 state. In the work of Gittins *et al.*,²⁷ the first excited state was studied in a supersonic jet using fluorescence excitation and two-color REMPI, and 32 modes were assigned based on their configuration interaction singles (CIS) calculation. However, as will be discussed later, the authors did not distinguish the two closely coupled electronic states explicitly, and there might be some complications with the calculation procedure. Additional IR spectroscopy of BaP and its radical ion was reported from doped wax films and argon matrices²⁸ between 400 and 2000 cm^{-1} .

EXPERIMENTAL SETUP

The experimental apparatus is a differentially pumped high vacuum molecular beam machine, with the detection chamber enclosed inside the source chamber.^{16–18} The sample BaP (Aldrich) was housed and heated to $170 \text{ }^\circ\text{C}$ in the pulsed valve located in the source chamber to achieve sufficient vapor pressure. The vapor was seeded in 1600 torr of argon and co-expanded into vacuum through a pulsed valve with a 1 mm orifice. After passing through a 2 mm skimmer, the cooled sample reached the detection chamber for laser excitation and ionization. The laser systems included two Nd:YAG (Spectra Physics, GCR 190 and GCR 230) pumped dye lasers (Laser Analytical System, LDL 20505 and LDL 2051). The excitation laser in the 398–382 nm range (Exalite 389) had a pulsed energy of 1.5 mJ/pulse with a bandwidth of 0.5 cm^{-1} . The ionization laser in the 312.3–304.6 nm range from the frequency-doubled dye laser (Rhodamine 610 and sulforhodamine 640) had a pulse energy of 1 mJ/pulse with a bandwidth of 0.3 cm^{-1} . The absolute wavelength of each laser was calibrated using an iron hollow-cathode lamp filled with neon. The relative timing between the two laser pulses was controlled by two delay generators (Stanford Research, DG 535), and the optimal signal was obtained under temporal overlap between the pump and ionization lasers. In the ZEKE experiment, molecules excited to high Rydberg states were allowed to stay for 1–2 μs in the presence of a constant dc spoiling field of $\sim 0.5 \text{ V/cm}$, after which ionization and extraction were achieved by a pulsed electric field of $\sim 5 \text{ V/cm}$.

GAUSSIAN 09 suite²⁹ was used to optimize the molecular structure and to obtain vibrational frequencies for assignment of the observed vibronic structures from REMPI and ZEKE. For the ground state of the neutral and the cationic state, density functional theory (DFT) calculations using the B3LYP functional were performed with the 6-31+G (d,p) basis set. The excited state S_1 was calculated using the time-dependent density functional theory (TDDFT) with the 6-31G basis set.

RESULTS

Two-color 1+1' REMPI spectroscopy

The two-color 1+1' REMPI spectrum of BaP near the origin of the $S_1 \leftarrow S_0$ electronic transition is displayed in Figure 2. The ionization laser was set at 290 nm and was temporally overlapped with the scanning resonant laser. The most intense peak at $25\,205 \pm 3 \text{ cm}^{-1}$ is assigned as the origin band, which is 28 cm^{-1} to the red compared with the report by Gittins *et al.*²⁷ and 60 cm^{-1} to the red of Greenblatt *et al.*²⁶ The experimental uncertainty of 3 cm^{-1} is mostly due to the linewidth of the vibronic bands, since the linewidth of the excitation laser beam is only 0.5 cm^{-1} . Other observed vibronic transitions are listed in Table I. The labeling of each vibrational mode is based on spectroscopic conventions, i.e., by using consecutive numbers in reference to the symmetry species and the frequency in decreasing order. The listed theoretical values were obtained from our TDDFT calculations by setting the keyword “root = 2” in the input file, i.e., the nominally 2nd excited electronic state, and this choice will be discussed in the latter part of this section. The values include a scaling factor of 0.9633, which was derived from a least square linear regression method with a coefficient of determination (R^2) of 0.9983.

BaP is a planar molecule with C_s symmetry. There are altogether 90 vibrational normal modes, with 61 a' modes that are numbered 1–61, and 29 a'' modes numbered 62–90. Within the range of our REMPI spectrum, 13 of the a' modes should be observable, from mode 61 to mode 48, and these modes constitute the central cluster of vibronic transitions

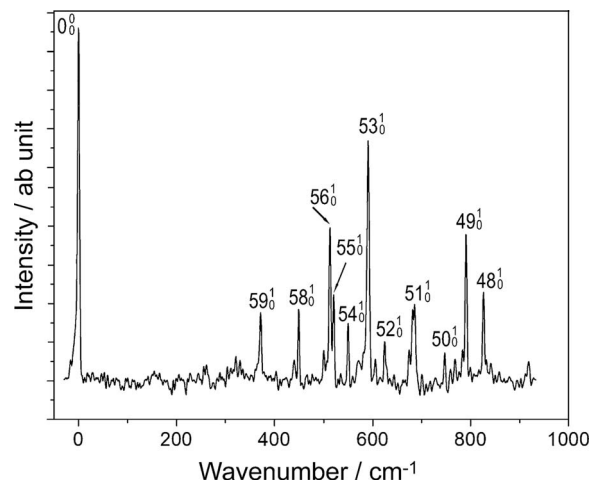


FIG. 2. REMPI spectrum of benzo[*a*]pyrene. The spectrum is shifted by $25\,205 \text{ cm}^{-1}$ —the origin of the $S_1 \leftarrow S_0$ transition—to emphasize the frequencies of the different vibrational modes of the S_1 state.

TABLE I. Observed and calculated vibrational frequencies of the S_1 state of benzo[a]pyrene.

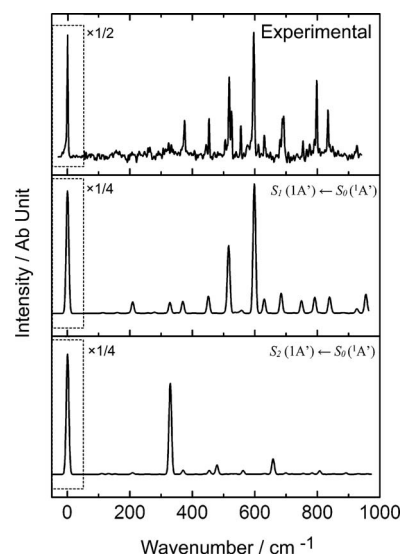
Experimental	Calculation (TDDFT) ^a	Assignment	Description of modes
373	369	59 ¹	Phenyl swing
451	451	58 ¹	Pyrene modes
515	505	56 ¹	Pyrene modes
523	515	55 ¹	Skeletal, longitudinal stretch
551	557	54 ¹	Pyrene modes
593	597	53 ¹	Skeletal, transverse stretch
626	629	52 ¹	Phenyl stretch
688	683	51 ¹	Skeletal
749	748	50 ¹	Pyrene modes
793	791	49 ¹	Pyrene modes
829	837	48 ¹	Skeletal

^aScaled by 0.9633.

in the spectrum. The intensities of the two lowest a' modes 60 and 61 are much weaker than those of other a' modes, and they are buried in the low frequency region leading to the major vibronic bands. Mode 57 at 473 cm^{-1} seems to be completely missing. With the exception of mode 56, the agreement between theory and experiment is within 8 cm^{-1} , somewhat larger than the experimental uncertainty of 3 cm^{-1} . The theoretical frequency for mode 56 is significantly lower than the experimental value. As will be observed in the ZEKE experiment, the same trend of disagreement persists for the same mode in the cation. Below 350 cm^{-1} , there are several weak bands that could be tentatively assigned as overtones or combination bands of out-of-plane a'' modes. These bands are barely above the noise level in the spectrum, hence their assignment is not listed in Table I.

The observed Franck-Condon allowed totally symmetric a' modes can be grouped into three categories. The first type are modes located mainly on the pyrene ring structure,¹⁷ including modes 58, 56, 54, 50, and 49. In particular, modes 58 and 50 have very similar displacement vectors as two of the b_{3g} modes of pyrene. Due to the additional ring (I, Fig. 1) attached to the pyrene moiety in BaP, both modes shift to lower frequencies by about 10% from those of pyrene. The second type of observed modes including modes 59 and 52 are related to the motion of the extra phenyl ring (I). Mode 59 involves swinging and mode 52 involves stretching of the extra phenyl ring. The third type of modes are skeletal modes of the whole molecular frame, including modes 55, 53, 51, and 48. Mode 55 is the longitudinal stretching mode, and mode 53 is the transverse stretching mode. Mode 55 and 53 are widely reported among PAHs, and the frequencies of which are observed to be inversely proportional to the dimension of the molecule.¹⁷ Consistent with this trend, the frequencies of both stretching modes in BaP are lower than those in pyrene. The rest of the skeletal modes involve mixed motions of stretching and ring deformation.

A typical complication in vibronic assignment of PAHs is caused by two closely spaced electronically excited states S_1 and S_2 .³⁰ Several work including our own have discovered that CIS and TDDFT calculations can sometimes predict the wrong order of states.^{17,31-33} For this reason, we calculated

FIG. 3. Calculations of the vibronic spectra using GAUSSIAN 09 for both the $S_1 \leftarrow S_0$ and the $S_2 \leftarrow S_0$ transitions.

the vibrationally resolved spectra for both transitions of $S_1 \leftarrow S_0$ and $S_2 \leftarrow S_0$ based on the Franck-Condon principle,³⁴ and the results are shown in Figure 3. The displacement vectors and vibrational frequencies were taken from the output files of GAUSSIAN 09:²⁹ root = 2 for S_1 and root = 1 for S_2 . It is evident from Fig. 3 that the simulation of $S_1 \leftarrow S_0$ agrees with the experimental result in both line positions and intensity distribution. As for the simulation of the $S_2 \leftarrow S_0$ transition, the disagreement further confirms our assignment of the S_1 electronic state and the observed vibrational bands. It is worth noting that among the three PAHs that we have investigated,¹⁶⁻¹⁸ BaP is the first case when we used the newly available vibronic coupling feature of GAUSSIAN 09 to calculate the REMPI spectrum. The remarkable agreement in this case and the disagreements of our previous work on tetracene, pentacene, or pyrene testify to the importance of vibronic coupling in PAHs.

ZEKE spectroscopy

By scanning the ionization laser while setting the resonant laser at one of the intermediate vibronic states identified in the above REMPI experiment, we obtained pulsed field ionization ZEKE spectra as shown in Figures 4 and 5. The assignment of the vibrational levels of the cation is noted by a superscript “+.” The identification of the vibrational level of the intermediate state for each ZEKE spectrum is labeled in the corresponding panel by a black dot. The experimental and theoretical values are shown in Table II. Limited by the linewidth of the resonant transitions and the pulsed electric field, the uncertainty of the experimental values from ZEKE is 5 cm^{-1} . The calculation was performed at the B3LYP/6-31+G (d,p) level, and a scaling factor of 0.9803 was obtained from a least squares fitting procedure with a coefficient of determination of 0.9991. The agreement between theory and experiment is within a few wave numbers for most transitions below 1000 cm^{-1} , with the exception of a few transitions involving

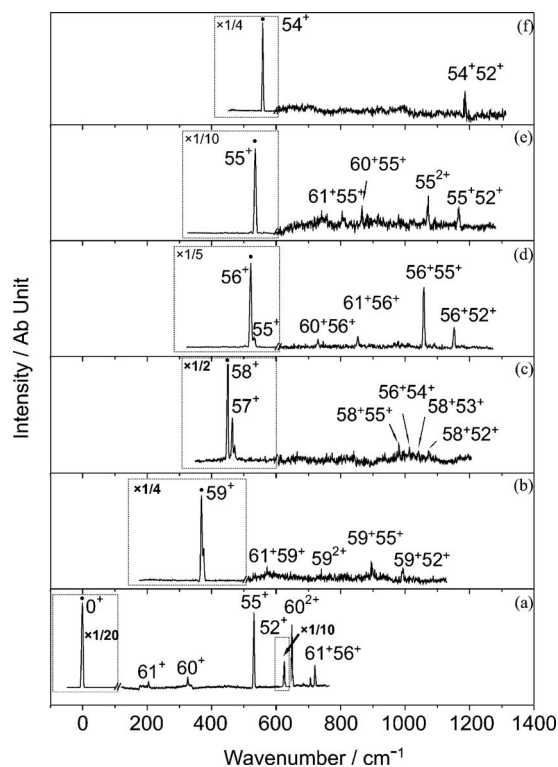


FIG. 4. Two-color ZEKE spectra of BaP recorded via the following vibrational levels of the S_1 state as intermediate states: (a) 0^0 , (b) 59^1 , (c) 58^1 , (d) 56^1 , (e) 55^1 , and (f) 54^1 . The energy in the figure is relative to the ionization threshold at $57\,271\text{ cm}^{-1}$. The assignment in the figure refers to the vibrational levels of the cation, and the corresponding vibrational level of the intermediate state is labeled by a black dot in each panel.

modes 55^+ and 56^+ . Higher frequency transitions are combination bands and overtones, which have larger deviations, particularly for bands with modes 55^+ and 56^+ . If we reset the frequencies of both modes 55^+ and 56^+ to be 10 cm^{-1} higher, the agreement between calculation and experiment in Table II would be within 10 cm^{-1} . In addition, because of the large number of possible combinations at high internal energies, some of these assignments are tentative. In several cases, the choice was made to preserve the vibrational mode of the intermediate state, and the rationale for this choice is the propensity rule, which will be discussed in the following. Nevertheless, the resulting assignment has yielded a consistent presence of combination bands with modes 55^+ and 52^+ regardless of the initial vibrational excitation.

The most striking feature of all the ZEKE spectra is the dominance of one vibrational band corresponding to the same vibrational excitation of the intermediate state. Unlike all the other PAH molecules we have studied,^{16–18} a clear propensity of preserving the vibrational excitation of the intermediate state can be identified in the ZEKE spectra of BaP, with negligible vibrational relaxation or mode mixing.^{35–39} When ambiguities arise in the assignment of combination bands, we therefore believe that the combination containing the original vibrational excitation is the most probable.

Figure 4(a) was recorded via the origin of the S_1 state, and the most intense peak corresponds to the origin of the cation. The adiabatic ionization potential is thus determined to be $57\,271 \pm 5\text{ cm}^{-1}$ ($7.1006 \pm 0.0006\text{ eV}$), taking into ac-

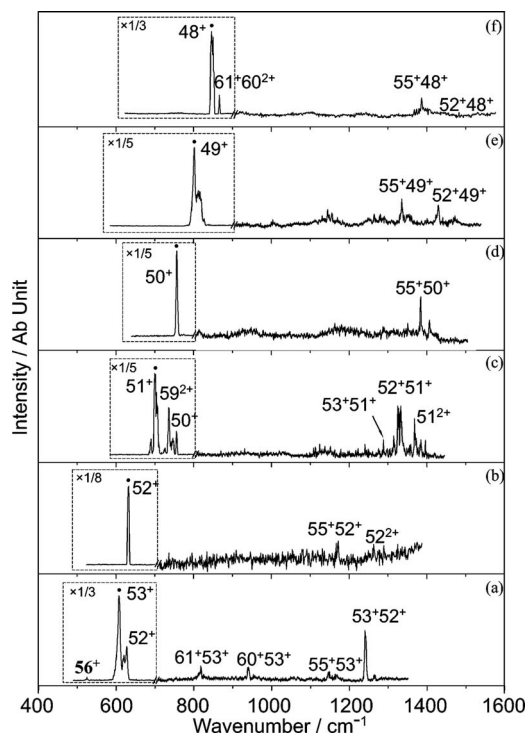


FIG. 5. Two-color ZEKE spectra of BaP recorded via the following vibrational levels of the S_1 state as intermediate states: (a) 53^1 , (b) 52^1 , (c) 51^1 , (d) 50^1 , (e) 49^1 , and (f) 48^1 . The energy in the figure is relative to the ionization threshold at $57\,271\text{ cm}^{-1}$. The assignment in the figure refers to the vibrational levels of the cation, and the corresponding vibrational level of the intermediate state is labeled by a black dot in each panel.

count the shift caused by the pulsed electric field. This value is 20 cm^{-1} lower than the ionization threshold extrapolated from the two-color REMPI experiment by Gittins *et al.*²⁷ The discrepancy is mostly related to the redshift of the origin of the S_1 state. In addition, a major vibrational band in Figure 4(a) is mode 52^+ , which is about $1/6$ of the intensity of the origin band (the unattenuated intensity distribution is shown Fig. 6(a)). All vibrational transitions with observable intensities in the ZEKE spectrum of Figure 4(a) correspond to excitations of a' modes. Both REMPI and ZEKE are governed by the Franck-Condon overlap, so if there are no major changes in the molecular frame upon electronic excitation and further ionization, the spectra of both Figs. 2 and Fig. 4(a) should have limited vibronic activities. Although not quantitative, the overall intensity distributions of the two spectra do look similar, with the exception of the overwhelming origin band and the mode 52^+ band of Fig. 4(a).

All ZEKE spectra were obtained from in-plane stretching modes, since the out-of-plane bending modes in the REMPI spectrum were too weak for further ZEKE experiments. None of the in-plane vibrational excitations of S_1 has activated any observable out-of-plane bending modes in ZEKE. Instead, a few limited stretching modes seem to have universal presence in the form of combination bands, such as modes 55^+ and 52^+ , thus the resulting ZEKE spectra have a similar intensity distribution, with a cluster of transitions between 500 and 700 cm^{-1} above the most intense transition. It is also interesting to notice that modes 60^+ and 61^+ are barely observable in

TABLE II. Observed and calculated vibrational frequencies of BaP cation.

Intermediate level in the S_1 state												Calc. ^a	Assignment
0^0	59^1	58^1	56^1	55^1	54^1	53^1	52^1	51^1	50^1	49^1	48^1		
0												0	0^{0+}
204												209	61^+
326												327	60^+
	369											372	59^+
		451										449	58^+
		472										476	57^+
			522	523		524						508	56^+
532			532	535								523	55^+
				561	554							557	54^+
	575											581	61^+59^+
						607						608	53^+
627						628	633					632	52^+
650												654	60^{2+}
								699				695	51^+
722			729					724				717	61^+56^+
				741				737				732	61^+55^+
	743							745				744	59^{2+}
								755	755			752	50^+
				803						803		808	49^+
						816						817	61^+53^+
											846	852	48^+
			852									837	60^+56^+
				867								852	60^+55^+
											866	863	61^+60^{2+}
	897											895	59^+55^+
							937					937	60^+53^+
		984										972	58^+55^+
	996											1004	59^+52^+
		1017										1006	58^+54^+
		1045										1053	58^+53^+
			1058									1031	56^+55^+
				1070								1046	55^{2+}
		1077										1081	58^+52^+
						1146						1131	55^+53^+
			1151									1140	56^+52^+
				1166				1169				1155	55^+52^+
					1181							1189	54^+52^+
						1239						1240	53^+52^+
							1260					1264	52^{2+}
								1290				1303	53^+51^+
								1329				1327	52^+51^+
										1335		1331	55^+49^+
								1370				1390	51^{2+}
									1383			1386	52^+50^+
											1387	1375	55^+48^+
										1430		1440	52^+49^+
											1484	1484	52^+48^+

^aScaled by 0.9803.

the REMPI spectrum, but they can be clearly identified in the ZEKE spectra of Figures 4(a), 4(d), and 5(a) as isolated bands and as combination bands. In addition, the missing mode 57^+ in the REMPI spectrum is now observed in the ZEKE spectrum through the excitation of mode 58 of the S_1 state in Figure 4(c). Altogether from modes 61^+ to 48^+ , the frequencies of the in-plane stretching modes of the cation are

spaced by 30–70 cm^{-1} , a situation prone to mode coupling and to complications in frequency assignment. The displacement vectors of the observed modes of the cationic state correlate with those from the S_1 state on a one-to-one basis, including the localized pyrene modes, the localized phenyl modes (ring I, Fig. 1), and the overall skeletal modes.

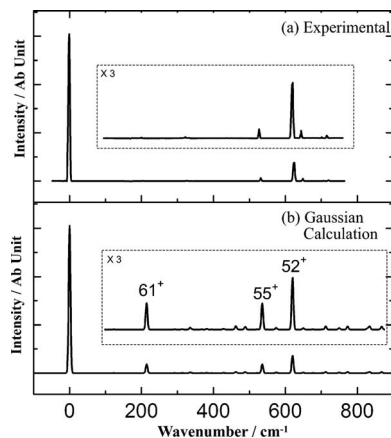


FIG. 6. Comparison between the experimental ZEKE spectrum from the origin of S_1 (a, reproduced from Fig. 4(a)) and (b) Franck-Condon simulation using GAUSSIAN 09.

DISCUSSION

Similar to pyrene, another peri-condensed PAH we have studied,¹⁷ BaP exhibits extensive configuration interactions, and in this situation, *ab initio* and DFT calculations typically fail to predict the correct order of the two nearby electronically excited states.^{32,33} The gap between the two lowest excited states of BaP is less than 2000 cm⁻¹ and both states have the same symmetry. The first excited electronic state S_1 with a relatively small oscillator strength is a mixed transition of LUMO+1 \leftarrow HOMO and LUMO \leftarrow HOMO-1, and the second excited state S_2 with a larger oscillator strength is a LUMO \leftarrow HOMO transition.⁴⁰ This type of energy level inversion has also been observed in pyrene.^{17,31,41–44} Consequently, to obtain the correct geometry and vibrational frequencies from either CIS or TDDFT calculations, we need to set the keyword “root = 2” in the input file. However, in comparing our results with those of Gittins *et al.*,²⁷ we discovered that there were substantial differences between the two calculations in both geometry and frequency. We then calculated the S_2 state by setting root = 1 using the same method, and reproduced the calculation result of Gittins *et al.* (all bond lengths in our results were shorter by about 0.003 Å–0.004 Å due to the higher basis set used in our calculation). Gittins *et al.* also pointed out that the Franck-Condon calculation based on their geometry file was in poor agreement with the experiment, opposite from our observation in Fig. 3. We therefore suspect that the assignment of Gittins *et al.* for the vibronic transitions in the REMPI spectrum was affected by the wrong keyword in the input file.

Although BaP has one additional ring compared with pyrene, and the two systems belong to different symmetry groups, it is still insightful to compare the vibrational modes of the two molecules. The extra ring (I) degrades the D_{2h} symmetry of pyrene to C_s for BaP. One would expect that BaP should have more flexibility and less rigidity than pyrene, and hence it should have more vibrational activities involving out-of-plane modes. In the REMPI spectrum of BaP (Fig. 2), however, the out-of-plane butterfly waving motions perhaps buried in the noise below 350 cm⁻¹ are overshadowed by the a' modes by orders of magnitude. This result is surpris-

ing since the corresponding out-of-plane modes in pyrene are on par with the Franck-Condon allowed bands.

The extremely weak out-of-plane modes if any in BaP might be related to the symmetry of the nearby S_2 state. Vibronic coupling with the S_2 (a') state in BaP does not expand the selection rule to out-of-plane modes. Similar Franck-Condon distributions might be possible for both S_1 and S_2 states in this case, and vibronic interaction might not change the spectral distribution to a noticeable degree. In contrast, the S_2 state of pyrene is ${}^1B_{1u}$, and vibronic coupling expands the selection rule to the out-of-plane b_{3g} modes. Thus, the intensity of out-of-plane modes or the degree of violation of the Franck-Condon principle might be more reflective of the molecular symmetry than that of the molecular rigidity.

The strong propensity for preserving the vibrational excitation of the intermediate level in ZEKE is an indicator of similarity in geometry between the intermediate state and the cation ground state. This point is further confirmed from the calculated geometries of the neutral ground state S_0 , the first excited state S_1 , and the cationic ground state D_0 . The overall change in size is within 0.5% of the linear dimensions of the molecular frame upon excitation or ionization. In contrast, for tetracene and pentacene, the width of the molecular frame increases by 1%–2% upon electronic excitation and shrinks back to nearly the same size as that of the original neutral ground state upon ionization.^{16,18} Although we have only a small set of samples, our studies of PAHs (Refs. 16–18) seem to suggest that highly symmetric species are easily deformed upon excitation or ionization, while low symmetry species have more ability to absorb the positive charge upon ionization.

We performed a Franck-Condon calculation using the GAUSSIAN suite²⁹ to simulate the $D_0 \leftarrow S_1$ transition from the origin of the S_1 state, and the results are shown in Figure 6. Similar to the experimental result, the origin band overwhelms the whole spectrum, in qualitative agreement with the experimental observation, and mode 52⁺ is the most intense vibrational band in the ZEKE spectrum. However, the agreement is not quite quantitative, and the intensities of modes 61⁺ and 55⁺ are overestimated in the calculation. We have also used a program from Dr. Dongsheng Yang for the same calculation^{34,45} and obtained the same qualitative agreement, although some details in the weak vibronic structures differ.

An interesting question for the cationic state is the location of the positive charge. We have calculated the Mulliken charge distribution and performed the natural population analysis for the S_0 and D_0 states, by including the charges on the peripheral hydrogen atoms in the adjacent rings and dividing the charges on the shared carbon atoms among conjoint rings. The results from the two types of charge analysis differ, but the change upon ionization is consistent: the positive charge of the cation is by no means localized in the phenyl group ring I or the pyrene group, and all rings share about the same amount of charge loss. Although we can categorize the observed vibrational modes into phenyl modes, pyrene modes, and skeletal modes, the fact that all three categories are observed with similar intensities supports the calculation result of a delocalized charge. Based on our calculation, C8 is the most positively charged among all the carbon atoms

connected with a hydrogen atom, and interestingly C8 is the most favorable for nucleophilic substitutions in organic chemistry.

All a' modes are IR active, hence our results of BaP can directly assist with line identification in astrophysical surveys. Khan and Dwayyan²⁸ studied the IR spectrum of BaP cation doped in a wax film as well as in an argon matrix from 400 cm^{-1} to 2000 cm^{-1} . Four a' modes 59⁺, 55⁺, 54⁺, and mode 50⁺ from the Khan and Dwayyan report are within our scanning range. The frequencies in wax films are 5 cm^{-1} higher than our values, but are still within our experimental uncertainty. Our work has further extended the experimental observation to below 400 cm^{-1} , including more than ten IR allowed modes of the cation and some of their overtones. In addition, some of the observed modes are discovered to deviate from DFT calculations by over 10 cm^{-1} , and the need of a scaling factor is also troublesome. This situation calls for precautions in relying exclusively on theoretical predictions for astrophysical fingerprints of PAHs.

CONCLUSION

Spectroscopic properties of electronically excited and ionic states of BaP have been studied using 1+1' two-color REMPI and two-color ZEKE. The observed vibronic transitions in the REMPI spectrum qualitatively agree with the Franck-Condon principle, dominated by in-plane stretching and bending modes. This result is different from that of pyrene, a PAH with one fewer ring but a much higher symmetry point group. The lack of or weak out-of-plane waving modes in BaP is a result of the same symmetry of the interfering S_2 state as that of the S_1 state. Consequently, the vibrational selection rule does not relax or expand to other types of modes even when vibronic coupling is present. The intensity of the out-of-plane modes is therefore reflective of the molecular symmetry, not indicative of the rigidity of the molecular frame. In addition, our TDDFT calculation using the GAUSSIAN 09 suite²⁹ with the 6-31G basis set is incapable of predicting the energy order of the two interfering electronic states, and the need to artificially "tweak" the calculation is also exemplified. For the cationic state, all observed vibrational modes are IR active, and with the exception of two modes, the DFT calculation, after scaling by a factor of 0.9803, are in agreement with the experimental data. However, the necessity of the scaling factor and the inability to predict all modes with the same accuracy raise the issue of reliability of DFT calculations. The limit of our calculation methods further calls for laboratory experimental efforts, particularly in the context of astrophysical studies. In this favorable case of BaP, ZEKE offers direct information for astrophysical line identifications.

ACKNOWLEDGMENTS

This work is supported by the National Aeronautics and Space Administration under Award No. NNX09AC03G.

¹F. C. Gillett, W. J. Forrest, and K. M. Merrill, *Astrophys. J.* **183**, 87 (1973).

²L. J. Allamandola, A. G. G. M. Tielens, and J. R. Barker, *Astrophys. J.* **290**, L25 (1985).

³D. A. Beintema, M. E. van den Ancker, F. J. Molster, L. B. F. M. Waters, A. G. G. M. Tielens, C. Waelkens, T. de Jong, T. de Graauw, K. Justtanont, I. Yamamura, A. Heras, F. Lahuis, and A. Salama, *Astron. Astrophys.* **315**, L369 (1996).

⁴A. Léger and J. L. Puget, *Astron. Astrophys.* **137**(1), L5 (1984).

⁵C. Moutou, A. Léger, and L. D'Hendecourt, *Astron. Astrophys.* **310**, 297 (1996).

⁶J. D. T. Smith, D. A. Dale, L. Armus, B. T. Draine, D. J. Hollenbach, H. Roussel, G. Helou, R. C. Kennicutt, A. Li, G. J. Bendo, D. Calzetti, C. W. Engelbracht, K. D. Gordon, T. H. Jarrett, L. Kewley, C. Leitherer, S. Malhotra, M. J. Meyer, E. J. Murphy, M. W. Regan, G. H. Rieke, M. J. Rieke, M. D. Thornley, F. Walter, and M. G. Wolfire, *Astrophys. J., Suppl. Ser.* **154**, 199 (2004).

⁷J. D. T. Smith, B. T. Draine, D. A. Dale, J. Moustakas, J. R. C. Kennicutt, G. Helou, L. Armus, H. Roussel, K. Sheth, G. J. Bendo, B. A. Buckalew, D. Calzetti, C. W. Engelbracht, K. D. Gordon, D. J. Hollenbach, A. Li, S. Malhotra, E. J. Murphy, and F. Walter, *Astrophys. J.* **656**(2), 770 (2007).

⁸A. G. G. M. Tielens, *Annu. Rev. Astron. Astrophys.* **46**(1), 289 (2008).

⁹S. R. Langhoff, *J. Phys. Chem.* **100**(8), 2819 (1996).

¹⁰G. C. Sloan, T. L. Hayward, L. J. Allamandola, J. D. Bregman, B. DeVito, and D. M. Hudgins, *Astrophys. J.* **513**, L65 (1999).

¹¹D. M. Hudgins, C. W. Bauschlicher, L. J. Allamandola, and J. C. Fetzer, *J. Phys. Chem. A* **104**(16), 3655 (2000).

¹²M. Vala, J. Szczepanski, F. Pauzat, O. Parisel, D. Talbi, and Y. Ellinger, *J. Phys. Chem.* **98**(37), 9187 (1994).

¹³H. S. Kim, D. R. Wagner, and R. J. Saykally, *Phys. Rev. Lett.* **86**(25), 5691 (2001).

¹⁴F. Qi, R. Yang, B. Yang, C. Huang, L. Wei, J. Wang, L. Sheng, and Y. Zhang, *Rev. Sci. Instrum.* **77**(8), 084101 (2006).

¹⁵L. Biennier, F. Salama, M. Gupta, and A. O'Keefe, *Chem. Phys. Lett.* **387**(4-6), 287 (2004).

¹⁶J. Zhang, L. Pei, and W. Kong, *J. Chem. Phys.* **128**(10), 104301 (2008).

¹⁷J. Zhang, F. Han, and W. Kong, *J. Phys. Chem. A* **114**(42), 11117 (2010).

¹⁸J. Zhang, F. Han, A. Li, and W. Kong, *Astrophys. J.* **715**(1), 485 (2010).

¹⁹A. Li, in *Deep Impact as a World Observatory Event: Synergies in Space, Time, and Wavelength*, edited by H. U. Kaufl, R. Siebenmorgen, and A. F. M. Moorwood (Springer, Berlin, 2009), p. 161.

²⁰A. Li and J. I. Luning, *Astrophys. J.* **594**, 987 (2003).

²¹M. F. Denissenko, A. Pao, M.-S. Tang, and G. P. Pfeifer, *Science* **274**(5286), 430 (1996).

²²E. Kriek, M. Rojas, K. Alexandrov, and H. Bartsch, *Mutat. Res. Fundam. Mol. Mech. Mugag.* **400**(1-2), 215 (1998).

²³L. E. Smith, M. F. Denissenko, W. P. Bennett, H. Li, S. Amin, M.-S. Tang, and G. P. Pfeifer, *J. Natl. Cancer Inst.* **92**(10), 803 (2000).

²⁴W. E. Bachmann and J. M. Chemerda, *J. Am. Chem. Soc.* **60**, 1023 (1938).

²⁵T. Imasaka, H. Fukuoka, T. Hayashi, and N. Ishibashi, *Anal. Chim. Acta* **156**, 111 (1984).

²⁶G. D. Greenblatt, E. Nissani, E. Zaroura, and Y. Haas, *J. Phys. Chem.* **91**(3), 570 (1987).

²⁷C. M. Gittins, E. A. Rohlfing, and C. M. Rohlfing, *J. Chem. Phys.* **105**(17), 7323 (1996).

²⁸M. N. Khan and A. A. Dwayyan, *Can. J. Pure Appl. Sci.* **3**(2), 833 (2009).

²⁹M. J. Frisch, G. W. Trucks, H. B. Schlegel *et al.*, GAUSSIAN 09, Revision B.01, Gaussian, Inc., Wallingford, CT, 2009.

³⁰E. Clar, *Polycyclic Hydrocarbons* (Academic, New York, 1964).

³¹M. Dierksen and S. Grimme, *J. Chem. Phys.* **120**(8), 3544 (2004).

³²M. Parac and S. Grimme, *Chem. Phys.* **292**(1), 11 (2003).

³³J. V. Goodpaster, J. F. Harrison, and V. L. McGuffin, *J. Phys. Chem. A* **102**(19), 3372 (1998).

³⁴D.-S. Yang, M. Z. Zgierski, D. M. Rayner, P. A. Hackett, A. Martinez, D. R. Salahub, P.-N. Roy, and T. Carrington, *J. Chem. Phys.* **103**(13), 5335 (1995).

³⁵Y. He and W. Kong, *J. Chem. Phys.* **124**(20), 204306 (2006).

³⁶Y. He, C. Wu, and W. Kong, *J. Chem. Phys.* **121**(17), 8321 (2004).

³⁷Y. He, C. Wu, and W. Kong, *Chem. Phys. Lett.* **391**(1-3), 38 (2004).

³⁸Y. He, C. Wu, and W. Kong, *J. Chem. Phys.* **121**(8), 3533 (2004).

³⁹C. Wu, Y. He, and W. Kong, *Chem. Phys. Lett.* **398**(4-6), 351 (2004).

⁴⁰J. B. Birks, *Photophysics of Aromatic Molecules* (Wiley, London, 1970).

⁴¹S. Grimme, *Chem. Phys. Lett.* **259**(1-2), 128 (1996).

⁴²Y. Bito, N. Shida, and T. Toru, *Chem. Phys. Lett.* **328**(3), 310 (2000).

⁴³J. Tanaka, *Chem. Soc. Jpn. Bull.* **38**(1), 86 (1965).

⁴⁴N. A. Borisevich, L. B. Vodovatov, G. G. D'yachenko, V. A. Petukhov, and M. A. Semyonov, *J. Appl. Spectrosc. (USSR)* **62**(3), 482 (1995).

⁴⁵D.-S. Yang, *Coord. Chem. Rev.* **214**(1), 187 (2001).